Pediatric RESEARCH

www.nature.com/pr

BASIC SCIENCE ARTICLE

The TGF-β1 pathway is early involved in neurogenic bladder fibrosis of juvenile rats

Yan Chen[1,2], Yuan Ma[1,2], Yulin He[1,2], Dong Xing[1,2], Erpeng Liu[1,2], Xinghuan Yang[1,2], Wen Zhu[3], Qingwei Wang[3] and Jian Guo Wen[1,2]

BACKGROUND: This study investigated whole neurogenic bladder's progression changes, as well as the expression of TGF-β1 fibrosis pathway-related proteins in bilateral spinal nerve-amputated juvenile rats.

METHODS: Sixty-four 8-week-old rats (32 bilateral L6 + S1 spinal nerve amputated and 32 sham operated) were selected. Cystometry was performed. General assessments, Masson, Sirius red, immunohistochemical staining, and western blotting of fibrosis and TGF-β1 pathway-related proteins were conducted using bladder tissues.

RESULTS: Cystometry results showed that the basal intravesical pressures and bladder capacities in nerve-amputated rats were significantly higher than those in sham-operated ones. Compared to the sham-operated groups, the bladder size and wall thickness in the nerve-amputated groups increased initially but then decreased over time. However, bladder weight continuously increased over time. Disintegration, thickening, and hypertrophy of the bladder wall were found over time in the amputated rats. Moreover, there was a significant increase in collagen III, and the ratio of collagen III/I was higher in amputated rats ($P < 0.01$). Finally, the expression of TGF-β1, TGF-βRI, Smad2, and collagen III and I increased in amputated bladder tissues, while Smad6 decreased over time.

CONCLUSIONS: The main clinical features of pediatric neurogenic bladder (PNB) were detrusor paralysis and continuous intravesical pressure. Biological molecular findings are earlier than the pathophysiological findings. Therefore, early preventing bladder fibrosis by targeting TGF-β1/Smad pathway-related proteins once knowing the PNB diagnosis might be an alternative treatment for PNB.

Pediatric Research (2021) 90:759–767; https://doi.org/10.1038/s41390-020-01329-x

IMPACT:

- The study found that the main clinical features of PNB were detrusor paralysis, continuous intravesical pressure, and increased TGF-beta/Smad signal proteins over time.
- The study makes contributions to the literature because it suggests biological molecular findings are earlier than the pathophysiological findings by various staining in PNB.
- The study investigated whole neurogenic bladder's progression changes, as well as the expression of TGF-β1 fibrosis pathway-related proteins in the spinal nerve-injured PNB juvenile rat models, which suggests that early prevention of bladder fibrosis by targeting TGF-β1/Smad pathway-related proteins once knowing the PNB diagnosis might be an alternative treatment for pediatric neurogenic bladder.

INTRODUCTION

Pediatric neurogenic bladder (PNB) is the progressive bladder dysfunction caused by impaired urinary sensible or voiding nerves, mostly due to various spinal nerves abnormality, ultimately resulting in renal dysfunction.[1,2] The prevalence of PNB is from 0.45 to 2.6% in children.[3] PNB often leads to serious bladder dysfunction in children, such as decreased bladder compliance, increased intravesical pressure, delayed emptying, and other serious bladder dysfunction, manifested as urinary incontinence, dysuria, repeated urinary tract infection, upper urinary tract damage, seriously life-threatening to patients, causing great pain to patients and their families, seriously affecting work and study, and increasing social burden.[4]

Current medical management for PNB, such as clean intermittent catheterization, antimuscarinic drugs like oxybutynin, intravesical injection of biotoxins, and bladder augmentation surgery, can effectively relieve patients' symptoms, but has little effect to prevent or delay the PNB bladder's deterioration on functions and morphologies.[5] Neuroanastomosis treatment for PNB has attracted worldwide attention recently,[6] but its therapeutic effect is controversial, and its clinical application is limited.[7] Our previous studies found that the bladder function

[1]Pediatric Urodynamic Center and Department of Pediatric Surgery, The First Affiliated Hospital of Zhengzhou University, 450052 Zhengzhou, China; [2]Institute of Clinical Medicine, The First Affiliated Hospital of Zhengzhou University, 450052 Zhengzhou, China and [3]Department of Urology, The First Affiliated Hospital of Zhengzhou University, 450052 Zhengzhou, China
Correspondence: Jian Guo Wen (wenjg1963@163.com)
These authors contributed equally: Yan Chen, Yuan Ma.

Received: 17 September 2020 Revised: 22 November 2020 Accepted: 30 November 2020
Published online: 19 January 2021

could not be fully recovered after lumbosacral nerve transection and neurogenic bladder nerve anastomosis and recanalization, and bladder fibrosis occurred in PNB bladder over time.[8] It is speculated that bladder fibrosis is an important factor affecting the therapeutic effect.[9] Therefore, successful treatment of PNB requires not only restoration of bladder innervation but also prevention and treatment of bladder fibrosis. However, the mechanism of PNB bladder fibrosis is still unclear, and there is no ideal treatment. Therefore, it is necessary to strengthen the basic and clinical research of PNB fibrosis.

To clarify when and how bladder fibrosis occurs during PNB progression, we used juvenile Sprague-Dawley (SD) rats to create PNB models by cutting the bilateral lumbar 6 (L6) and sacral 1 (S1) spinal nerves, which simulate PNB caused by lumbosacral spina bifida or lumbosacral spinal cord and/or spinal nerve dysplasia in children,[10,11] and then we investigated whole neurogenic bladder's progression changes like morphology, structure, and function, as well as the expression of transforming growth factor (TGF)-β1 fibrosis pathway-related proteins in the PNB rat models, which might help to elucidate the whole molecular mechanism of PNB development and suggest better treatment strategy.

EXPERIMENTAL

Animals

Sixty-four 8-week-old healthy female juvenile SD rats (150 ± 9.6 g) were provided by the experimental animal center of the local Medical University. The animals were housed in the animal facility at 22 ± 1 °C with 45–55% relative humidity on a 12-h artificial light–dark cycle. The local medical ethical committee approved all animal procedures (approval number 2018-KY-86).

Experimental design

PNB juvenile rat model. The PNB juvenile rat models were created as previously described by cutting the bilateral lumbar 6 (L6) and sacral 1 (S1) spinal nerves, which simulate PNB caused by lumbosacral spina bifida or lumbosacral spinal cord and/or spinal nerve dysplasia in children.[10,11] In brief, after inhalation anesthesia with 2% isoflurane (R51022,WEST GENE, Shanghai china), a dorsal median incision was created to expose the dorsal and ventral roots of L6–S1. The ventral and dorsal roots of bilateral L6 and S1 were transected, and the root stumps were ligated and buried into an adjacent muscle to prevent spontaneous nerve regeneration. In the sham group, nerve roots were only exposed by surgical instruments without transection or any other operation. Animals were housed separately postoperatively and kept on a 37 °C heating blanket overnight. Food and water were available ad libitum. Penicillin (2×10^6 U/day) was administered for 3 days postoperatively.

Experimental groups. Rats were randomly divided into 8 groups (4 spinal nerve amputation and 4 sham groups) at 3-, 6-, 12-, and 24-week post-operation, and each group has 8 rats.

Cystometry

Cystostomy in juvenile rats. After the juvenile rats were anesthetized and underwent nerve amputation or sham operation, cystostomy was performed immediately as follows: a 1-cm incision (fist incision) was made on the midline extending cephalad above the pubic bone. A 6-0 silk suture was passed around the vertex of the bladder. A small incision was made within the suture limits, following which the PE50 catheter with a flared tip was passed into the bladder about 0.3 cm long, and the suture was tightened around the catheter (Fig. 1a). The bladder was flushed back and forth through the catheter to assure no leakage.

A second incision of around 0.5 cm in size and approximately 3.0 cm above the first incision and a third incision of about 1.0 cm in size at the posterior neck were made to create a subcutaneous tunnel. Subsequently, a trocar was passed through the abdominal muscles from these three incisions, and the PE50 catheter was then passed through the trocar. After removal of the trocar, the catheter emerged through the tunnel at the back of the neck and was fixed to the subcutaneous fascia tissue with a 4-0 silk thread (Fig. 1b). Less than 4.0 cm of the catheter was left outside the skin to prevent the rat from biting the distal end. The cystostomy catheter was checked and cleaned every day for cystometry, as needed.

Cystometry through cystostomy catheter. The cystostomy catheters in all groups were connected to a peristaltic pump (3M, Saint Paul, MN) (Fig. 1c) and urodynamic equipment (Dantec Menuet Electrons, Skovlunde, Denmark) via a three-way connector for both infusion and pressure recording (Fig. 1d). Cystometry was performed by infusing warm saline (37–38 °C) with filling rate 6 ml/h in shams and 15 ml/h in the PNB group, and basal intravesical pressure, bladder leak point pressure (BLPP), bladder compliance, maximum cystometric capacity, and maximum bladder contracting pressure were recorded. Three consecutive cystometries were performed in each rat, with an interval of at least 30 min to maintain consistent bladder activity.

Collagen fiber staining

Bladder samples were fixed with 10% paraformaldehyde buffer, dehydrated, and embedded in wax. The paraffin-embedded tissues were cut in 4-μm sections on a rotary microtome (Leica, RM2016). The paraffin sections were dewaxed and hydrated, followed by: (1) Masson staining, in which the microscopic examination showed the collagen fibers stained blue, while muscle fibers, fibrins, and red blood cells stained red; and (2) Sirius red staining, in which the collagen fibers were red, and the background was yellow under an optical microscope. However, under polarized light, collagen type III showed as a thin green fiber, and collagen type I as a thick orange or bright red fiber.

Immunohistochemical staining

Paraffin sections were dewaxed and rehydrated. Endogenous peroxidases were blocked using 0.5% H_2O_2 in methanol for 10 min at room temperature (RT, 20 °C), followed by antigen retrieval with 1 mM Tris/EDTA (pH 9.0) and blocking in phosphate-buffered saline (PBS) supplemented with 2% bovine serum albumin. Subsequently, samples were incubated overnight at 4 °C with the following primary antibodies: rabbit anti-TGF-β1 Rabbit pAb (GB11179, Servicebio, Wuhan, China), anti-Smad2 Rabbit pAb (GB11511, Servicebio), and anti-Smad6 Rabbit pAb (GB11654, Servicebio) diluted in PBS supplemented with 0.3% bovine serum albumin and 0.3% Triton X-100. After washing in PBS, the samples were incubated with horseradish peroxidase-conjugated secondary antibodies, and goat anti-rabbit immunoglobulin (GB23303, Servicebio) for 1 h at RT, followed by washing, antibody–antigen reaction with 0.05%3,3′-diaminobenzidine tetrachloride, and dissolving in distilled water containing 0.1% H_2O_2. Light microscopy was carried out using a Leica microscope. For each sample, at least ten randomly selected areas were evaluated.

Western blotting

Bladder tissues were dissected, ground, and lysed in the Mammalian Cell Protein Extraction Reagent (CWBiotech, Beijing, China). Total protein concentration was determined using the Pierce BCA Protein Assay Kit (Trans, Beijing, China). For each sample, 20 μg of protein was loaded and separated by sodium dodecyl sulfate–polyacrylamide gel electrophoresis. Subsequently, the proteins were electrophoretic transferred to a polyvinylidene fluoride membrane. The membranes were blocked with 5% nonfat milk in Tris-buffered saline (pH 7.4) containing 0.1% Tween-20 (TBST), incubated overnight at 4 °C with primary antibodies—rabbit anti-TGF beta receptor I (GB11271, Servicebio), anti-Smad2 (D43B4, Cell Signaling Technology, Danvers, MA), anti-Smad6

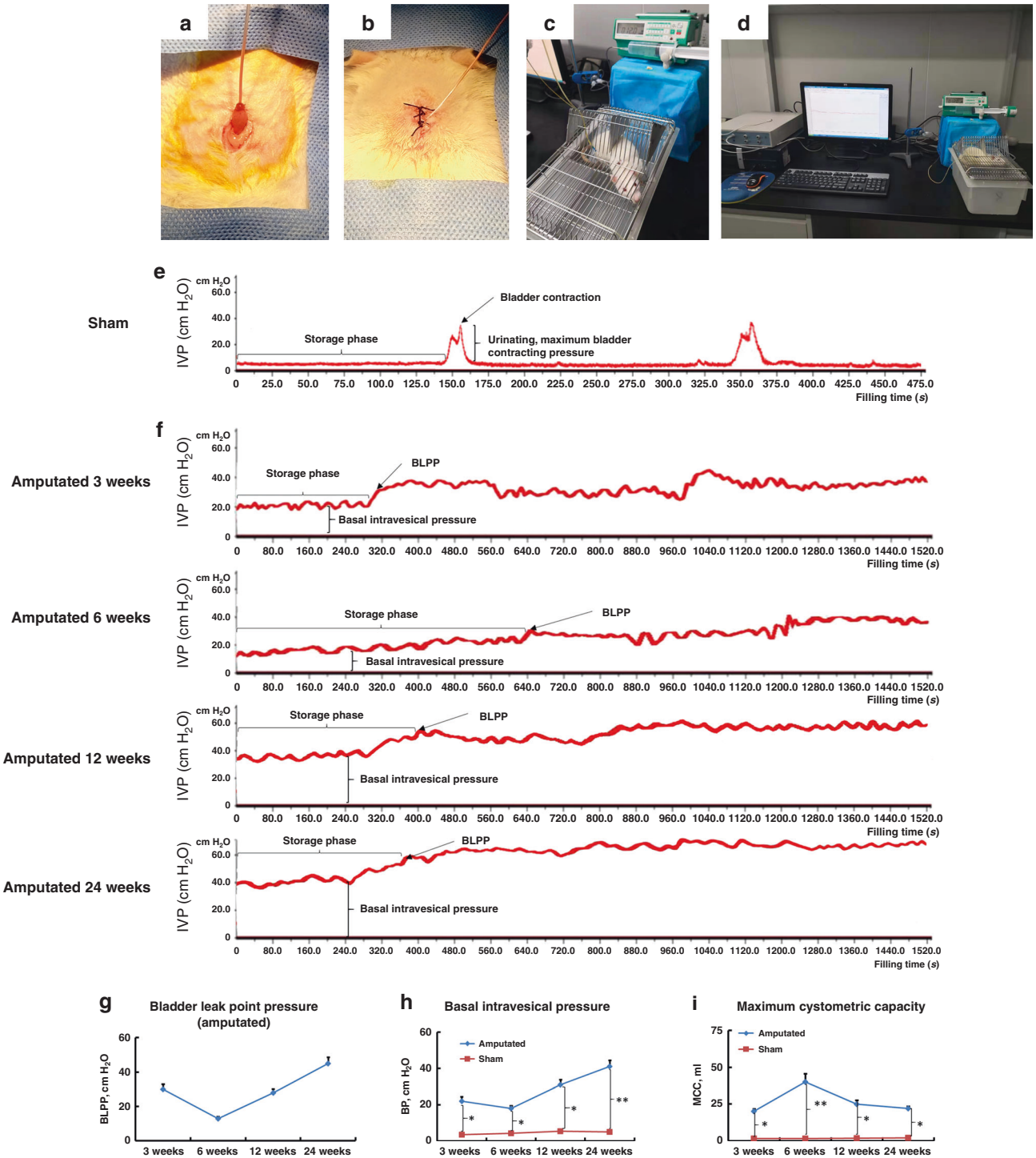

Fig. 1 Cystometry in spinal nerve-amputated and sham-operated rats. BLPP bladder leak point pressure, BP bladder basal pressure, MCC maximum cystometric capacity. Graph (**a**) showing cystostomy in the rats; Graphs (**b**, **c**, **d**) showing cystometry through cystostomy catheter in the rats; Graph (**e**) showing the cystometry profile in sham rats; Graph (**f**) showing the cystometry profile in amputated rats; Graph (**g**) showing the occurence and change of bladder leak point in amputated rats; Graphs (**h**–**i**) showing the comparison of cystometric parameters (basal intavisical pressure and maximum cyctometric capacity) in sham and amputated rats, $^{*}P \leq 0.05$, $^{**}P < 0.01$.

(PA5-87457, Invitrogen, ThermoFisher Scientific), anti-Collagen I (PA5-95137, ThermoFisher Scientific), and anti-Collagen III (PA5-34787, ThermoFisher Scientific)—in TBST with 5% nonfat milk. The secondary antibody (GB23303, Servicebio) was used to incubate the membrane for 2 h at RT. Labeling was performed using a western blot imaging with the Image Lab Software (ChemiDoc MP system, Bio-rad, Hercules, CA). Density and area of the bands were quantitated.

Statistical analysis

Calculations were performed using the GraphPad InStat3 for Macintosh software. Overall significance level between the

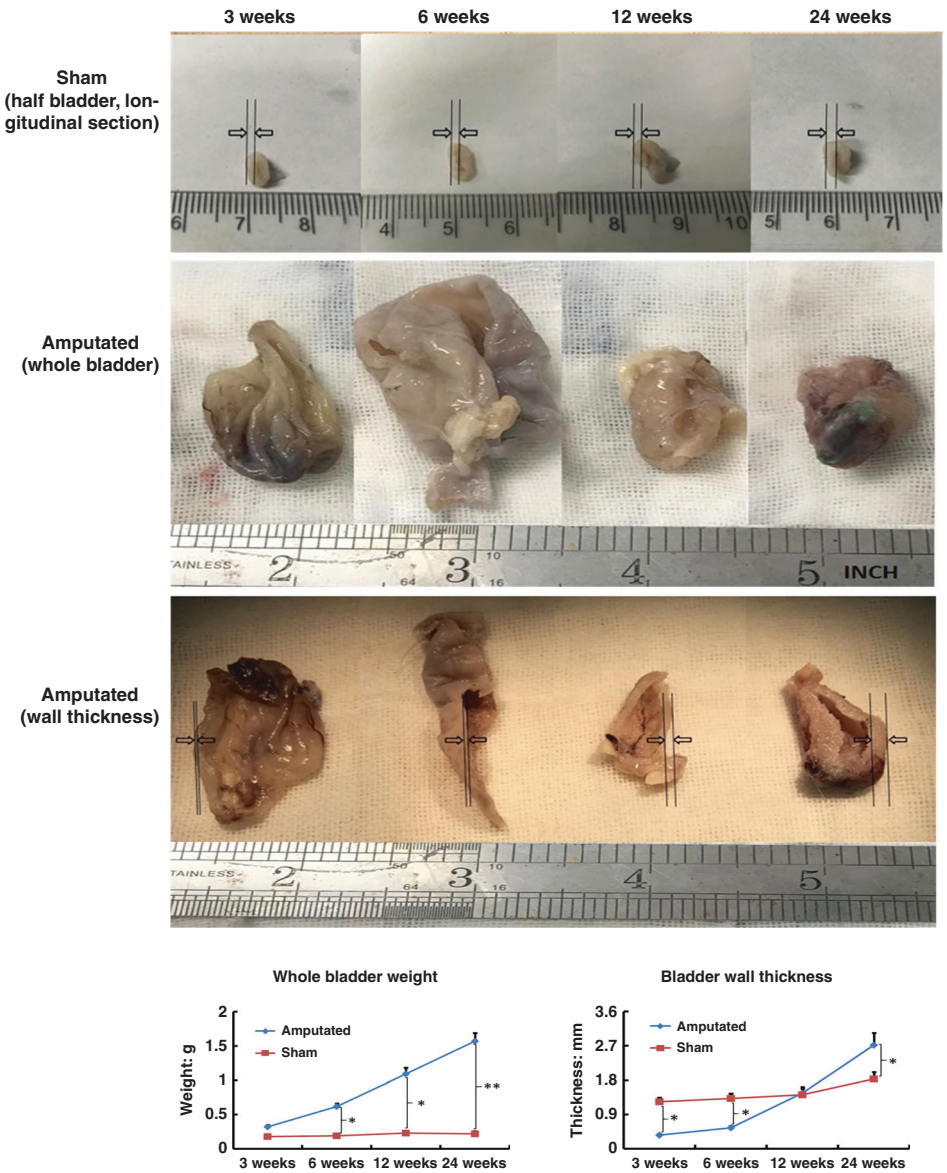

Fig. 2 Gross morphological changes of bladder tissue in spinal nerve-amputated and sham-operated rats. Longitudinal profile of sham-operated rats after 3, 6, 12, and 24 weeks (pictures showing half of the rat bladder) with bladder wall thickness (indicated by arrows) as 1.2, 1.3, 1.4, and 1.8 mm, respectively. Bladder wall thickness of the corresponding nerve-amputated rats was 0.36, 0.55, 1.46, and 2.72 mm, respectively. *$P \leq 0.05$, **$P < 0.01$.

amputated and sham groups or among the amputated groups was analyzed by one-way analysis of variance, using the Dunnett and Tukey–Kramer multiple comparison tests when appropriate. Statistical significance was set at $P < 0.05$. The data are shown as mean ± SEM.

RESULTS

Impaired cystometry in nerve-amputated rats

Cystometry showed no significant differences among the sham-operated groups at 3, 6, 12, and 24 weeks. Basal intravesical pressure was 3.51–5.42 cm H_2O with normal bladder compliance during filling. Further, bladder volume was 2.1 ± 0.04 mL, and maximum bladder contracting pressure was 40 ± 3.7 cm H_2O during voiding (Fig. 1e).

However, there was no obvious contracting/voiding phase in any of the spinal nerve-amputated groups. The BLPP occurred and increased in a time-dependent manner 6 weeks following the operation. Further, basal intravesical pressure and bladder volume significantly increased over time after 6 weeks post-operation in the nerve-amputated groups compared to the sham-operated group ($P < 0.05$; Fig. 1f–i).

Gross morphological changes of bladder tissue

The bladder size in the amputated groups initially increased at 3 and 6 weeks but decreased at 12 and 24 weeks when compared to the sham-operated groups. Further, the thickness of the bladder initially decreased at 3 and 6 weeks but gradually became thicker 6 weeks post-operation. Conversely, the bladder weight continuously increased over time in the nerve-amputated compared to the sham-operated groups (Fig. 2).

Disrupted bladder structure and increased collagen III in nerve-amputated rats

Masson staining showed that the normal connective tissues in the bladder wall disappeared in the amputated rats and the layered structure of the bladder gradually disintegrated. Further, the

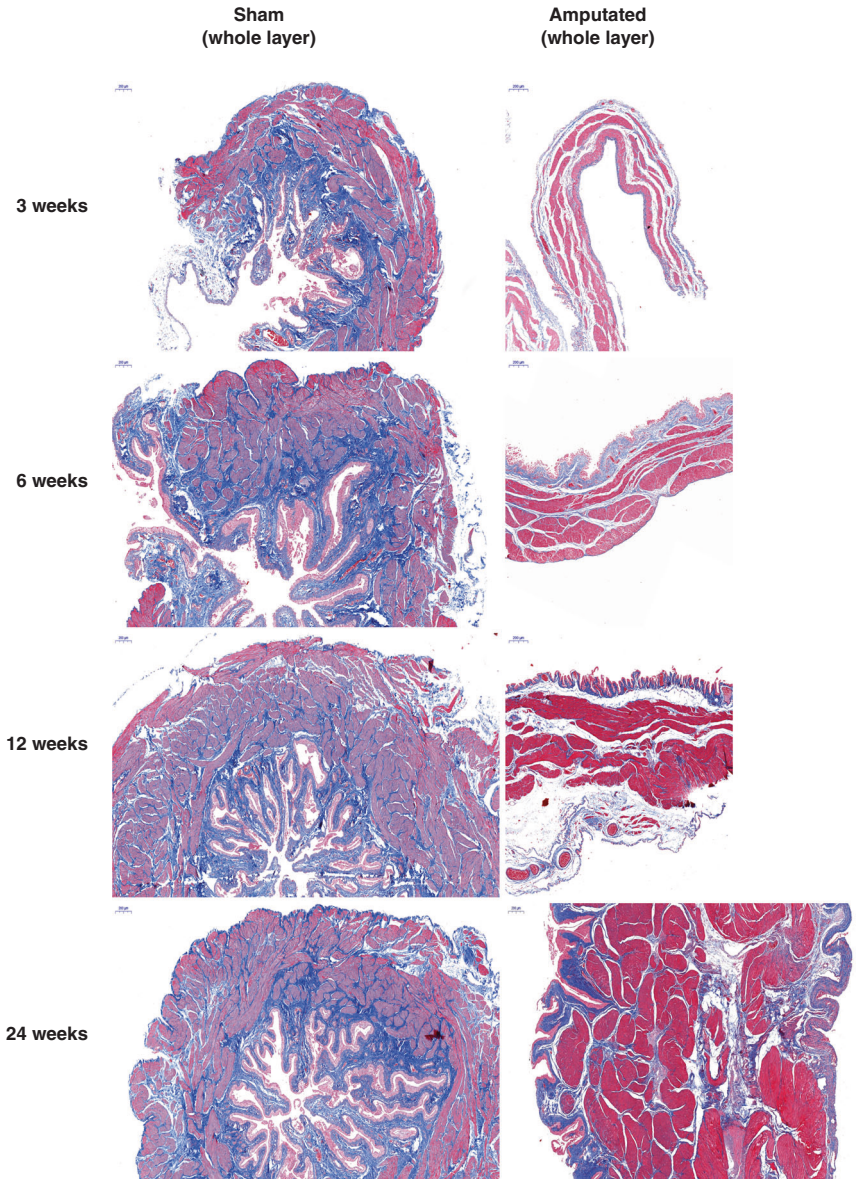

Fig. 3 Masson staining of whole layers of bladder tissue in spinal nerve-amputated and sham-operated rats. Scale bar, 200 μm.

thickness of the bladder wall initially became thinner, then gradually thicker. Additionally, the lamina propria decreased, the interstitial tissue became fibrillated, the smooth muscle tissues thickened and hypertrophied, and intramuscular collagen fibers gradually increased (Fig. 3).

Sirius scarlet staining of 3-, 6-, 12-week-amputated rat bladders showed no significant difference in collagen III and the ratio of type III/I collagen fibers, compared to related-sham groups (pictures not shown). But 24-week-amputated rat bladders by Sirius scarlet staining showed a significant increase in collagen III, and the ratio of type III/I collagen fibers was higher than the sham group (3.99 ± 0.91 vs. 0.87 ± 0.41; $P < 0.05$; Fig. 4).

Increased fibrosis-related protein expression in nerve-amputated rats

Immunohistochemical staining showed that expression of TGF-β1 and its classical pathway key protein Smad2 increased, while pathway inhibitory protein Smad 6 decreased, in the nerve-amputated groups when compared to the sham-operated groups (Fig. 5).

Further, western blot analysis showed that TGF-beta receptor I expression in the rat bladder of the 6-, 12-, or 24-week amputated groups was significantly higher than the sham group and increased over time ($P < 0.05$, $P < 0.01$; Fig. 6a, b). Smad2 expression in the 6-, 12-, or 24-week amputated groups was also significantly higher than the sham group and increased over time ($P < 0.05$, $P < 0.01$; Fig. 6a, c). Conversely, Smad6 expression was significantly lower than that in the sham group, decreasing over time ($P < 0.05$ or $P < 0.01$; Fig. 6a, d). Additionally, collagen I and collagen III expression levels in the 6-, 12-, or 24-week amputated groups were higher than the sham group and increased over time ($P < 0.05$, $P < 0.01$; Fig. 6a, c). However, collagen III increased more sharply, thus the ratio of collagen III/I increased in a time-dependent manner.

DISCUSSION

SD rats are often used to create neurogenic bladder animal models, which have advantages of high homozygosity within strains, strong regeneration, and anti-infection ability.[10,11]

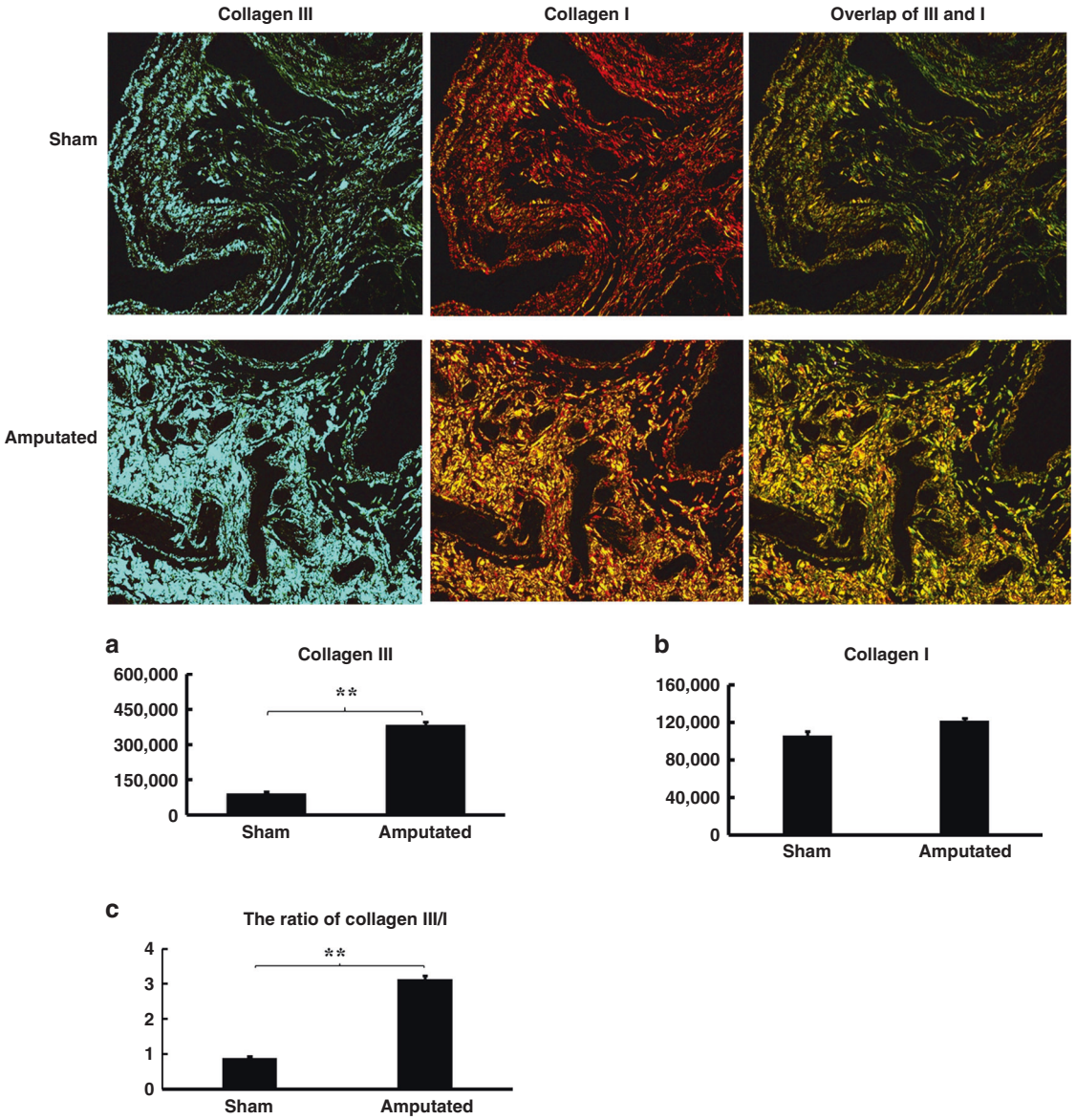

Fig. 4 Sirius Red staining of bladder tissue in 24-week spinal nerve-amputated and sham-operated rats. Representative images of 24-week sham (top) and nerve-amputated (bottom) rats. (Left) Type III collagen fibers under polarized lights (thin green fiber). (Center) Type I collagen fibers under polarized lights, shown as thick orange or bright red fibers. (Right) Mixture of type I and type III collagen fibers under polarized lights. Graphs (**a**–**c**) showing statistical comparison of type III (**a**), type I (**b**), and the ratio of III/I (**c**) collagen fibers between the sham and nerve amputation groups at 24 weeks. $^{**}P < 0.01$.

Twelve-week-old rats undergo sexual maturation and are usually defined as adult rats, and the cystometry parameters of bladder capacity, bladder basal pressure, and voiding pressure in the normal rats over 8-week-old changed very little with time. Thus we selected 8-week-old SD juvenile rats for the experiments to create the PNB animal model.

The main clinical features of PNB are detrusor paralysis and continuous high pressure of the bladder by cystometry.[12] Our PNB model by L6 + S1 amputation was also detrusor paralysis without obvious bladder contracting/voiding phase and continuous high pressure of the bladder by cystometry. In early stage of post-amputation (3-, 6-week post-amputation), the elevation of basal intravesical pressure was less significant than the middle- and late-stage of post-amputation (12-, 24-week post-amputation), which may be related to the compensatory bladder enlargement and bladder wall thinning as we observed (Figs. 2 and 3). While in the middle- and late-stage of post-amputation (12, 24 weeks), the basic intravesical pressure and BLPP become continuous significant higher pressure by cystometry (Fig. 1), which might result from thicker and harder bladder wall (Figs. 2 and 3). So our findings are similar to the current reports,[12] and made the more detailing supplements to the literature on the PNB cystometry changes.

Usually the pathophysiological changes of PNB are increased smooth muscle cell proliferation and extracellular matrix, collagen deposition, and bladder wall hypertrophy,[13] and it was reported that collagen I and III are the main collagens deposited during bladder fibrosis, with an increase in the type III/I ratio.[14] Our study also found the smooth muscle cell proliferation, extracellular matrix deposition, and bladder wall hypertrophy in the PNB rats obviously from 12-week post-amputation time by histochemical staining; but we only found collagen III deposition greatly and

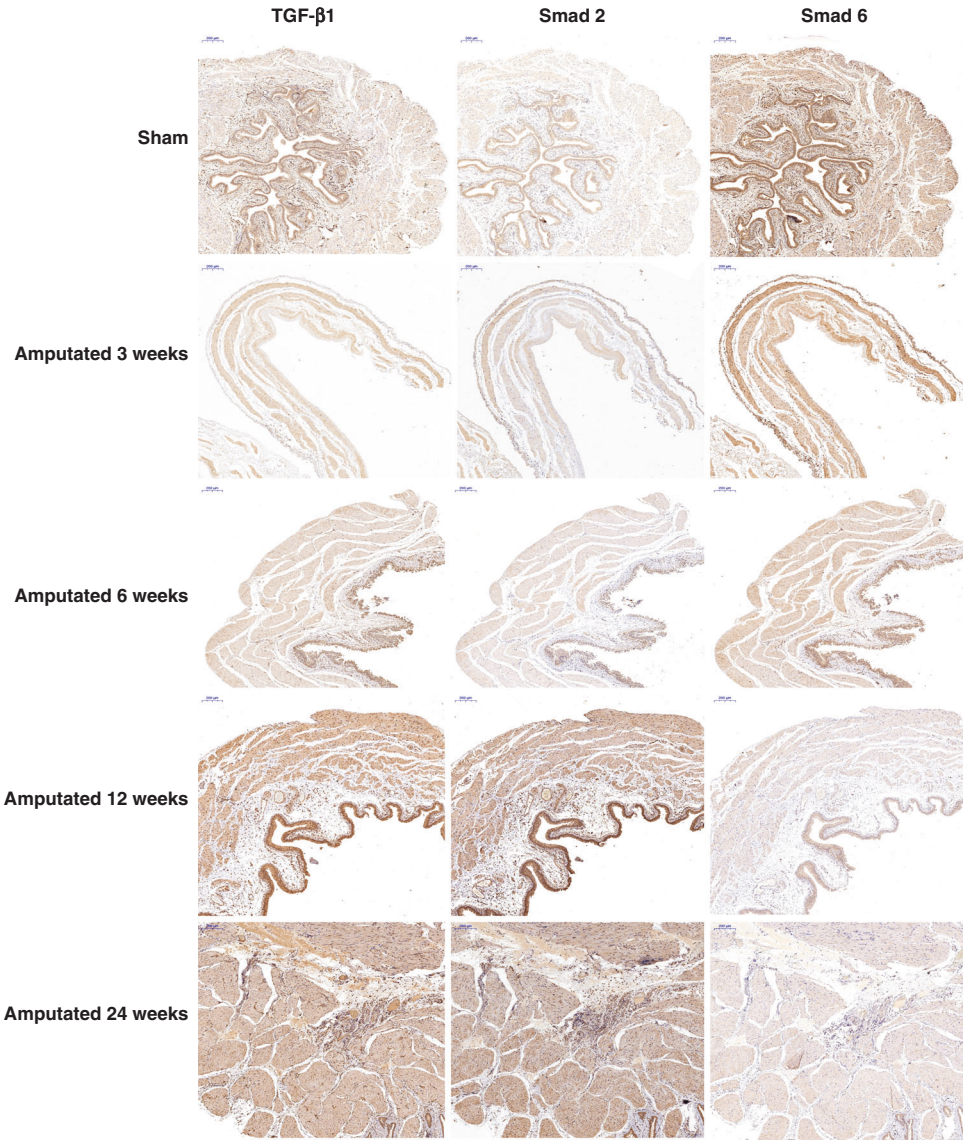

Fig. 5 Immunohistochemical staining of TGF-β1 pathway-related proteins TGF beta 1, Smad2, and Smad6 in bladder tissues of spinal nerve-amputated and sham-operated rats. Scale bar, 200 μm.

type III/I ratio increase from 24-week post-amputation by Sirius scarlet staining. However, molecular protein detection by western blot informed that both collagen III and collagen I proteins' expression levels increased from 12-week post-amputation, and the increase of collagen III protein was more and earlier from 6-week post-amputation, so the collagen III/I ratio increased progressively from 6-week post-amputation. In addition, protein expression levels of TGF-β1, Smad2, and TGF-beta receptor I also increased progressively from 6-week post-amputation in the PNB groups by western blot, while findings of protein increase by histochemical staining were from 12-week post-amputation.

Some studies reported TGF-beta/Smad signaling pathway was involved in chronic bladder outlet obstruction, causing bladder fibrosis.[15,16] The reason is that high intravesical pressure could be the extra harmful stimulus to bladder smooth muscle cells, in which the protein kinases could be further activated to regulate cell function changes and activate fibrosis progression.[15,16] In heart and liver researches, they reported the same findings that pressure overload induced myocardial fibrosis,[17] and stress activated protein kinases and initiated liver cells' fibrosis.[18] Our studies also found the fibrosis progression consistent with the intravesical pressure, especially with basal intravesical pressure, higher basal intravesical pressure, and severer fibrosis. It might be the constant high intravesical pressure initiating the fibrotic process, because high intravesical pressure started at least from 3-week post-amputation by cystometry, probably even earlier (Fig. 1), but the TGF-β1, Smad2, and TGF-beta receptor I and collagen III proteins increased progressively from 6-week post-amputation by western blot findings (Fig. 6). But these guesses needs further verification.

The effect of TGF-β1 on fibrosis is clear, and the fibrogenic effect of TGF-β1 is closely related to its receptors. Three receptors specifically bind to TGF beta 1, namely, TGF beta R I, TGF beta R II, and TGF beta R III, and the combinations of TGF beta 1 and TGF beta R I and II form a complex responsible for information transmission.[15,19] Smad2 protein has been reported to be the first activated downstream molecule transmitting TGF-β1 signals. TGF-β1 initiates its signaling pathway by mainly binding with TGF-beta receptor I on the cell membrane. This process phosphorylates and activates the intracellular Smad2 and Smad3 proteins to form a

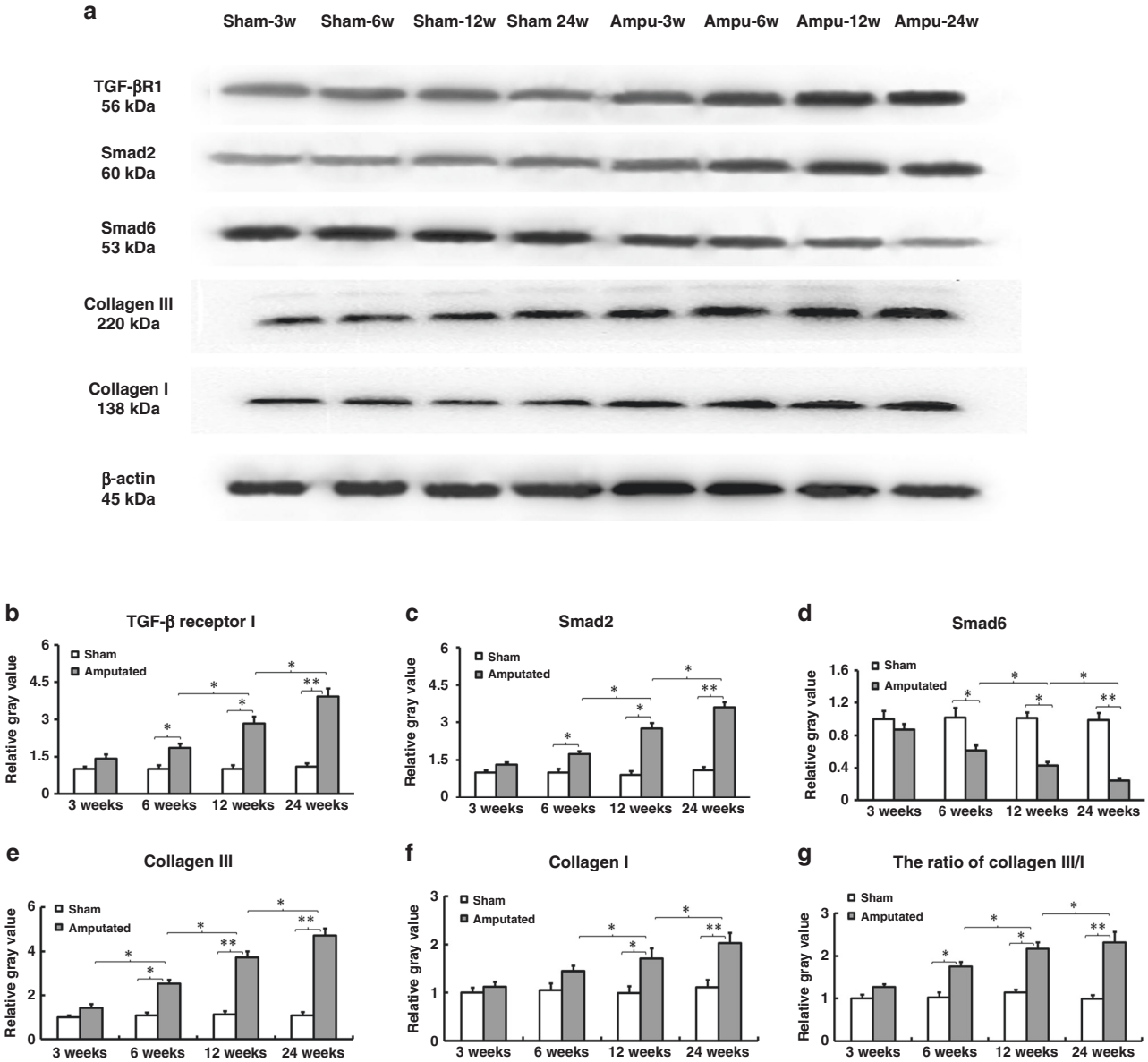

Fig. 6 TGF-beta receptor I protein expression in spinal nerve-amputated and sham-operated rats. a Representative western blots of TGF-beta receptor I, Smad2, Smad6, collagen III, and collagen I proteins ($n = 4$). Quantification of **b** TGF-beta receptor I, **c** Smad2, **d** Smad6, **e** collagen III, **f** collagen I, and **g** the ratio of collagen III/I protein expression. Data represent mean ± SD of 12 samples (3 repeated experiments using 4 samples each); $^{*}P \le 0.05$, $^{**}P < 0.01$.

complex, then transfers to the nucleus to regulate collagen and fibrin genes, induce extracellular matrix production, and increase expression of type I and III collagen proteins, stimulating cell hypertrophy and fibrosis.[19] Some researchers found decreased collagen deposition and increased bladder compliance in TGF-β1-deficient bladder outlet obstruction mice, also suggesting that TGF-β1 is involved in the process of cell fibrosis in the bladder.[20] In our study, we found that the expression of TGF-β1 and its downstream protein Smad2, together with collagen III and collagen I in bladder smooth muscle cells progressively increased over time after nerve amputation. In contrast, the pathway inhibitor protein Smad6 progressively decreased over time both by staining and western blot. Further, our findings on bladder morphology, structure, and function, e.g., thicker bladder wall, progressive collagen (primarily collagen III) deposition in the bladder tissues, and aggravated collagen III/I ratio, also pointed out the gross fibrotic appearance. These findings together implied that the TGF-β1/Smad signaling pathway gradually activate and progress over time in the PNB groups. Therefore, we suggest that effective treatment of neurogenic bladder in children should be started early before the occurrence of bladder fibrosis.

TGF-β1/Smad pathway inhibitors have been reported as fibrotic treatment in the liver, lung, heart, and kidney[15,21]; however, they have yet to be tested for bladder fibrosis. As such, future studies exploring TGF-β1/Smad pathway inhibitors to prevent fibrosis in neurogenic bladder are indeed needed, such as inhibition of Smad phosphorylation or TGF-β1 signal transmission using TGF-β1 receptor or other pathway protein inhibitors. We may explore these studies in the near future.

This study has some limitations, such as the rat model by cutting the bilateral lumbar 6 (L6) and sacral 1 (S1) spinal nerves, simulated PNB caused by lumbosacral spina bifida or lumbosacral spinal cord and/or spinal nerve dysplasia in children (the most common types in clinical practice).[10,11] Thus the model might not

apply to other PNB caused by brain diseases (e.g., brain hypoxia bladder) or peripheral nerves damages (e.g., diabetic bladder). Moreover, we selected 8-week-old SD juvenile rats for the experiments, so it gave less information about neurogenic bladder in infants or newborns.

In conclusion, our study found that the main clinical features of PNB were detrusor paralysis and continuous intravesical pressure at least from 3-week post-amputation by cystometry, probably even earlier; the smooth muscle cell proliferation, extracellular matrix deposition, bladder wall hypertrophy, and increased TGF-beta/Smad signal proteins in the PNB rats obviously from 12-week post-amputation time by pathophysiological staining, while TGF-beta/Smad signaling protein expression level changes were found from 6-week post-amputation time. Thus biological molecular findings are earlier than the pathophysiological findings by various staining. Therefore, early prevention of bladder fibrosis by targeting TGF-β1/Smad pathway-related proteins once knowing the PNB diagnosis might be an alternative treatment for PNB.

ACKNOWLEDGEMENTS

This work was supported by the National Natural Science Foundation of China (Grant numbers: U1904208 and 81670689). The funders had no role in the study design, data collection and analysis, decision to publish, or preparation of the manuscript.

AUTHOR CONTRIBUTIONS

Y.C. and Y.M. conceived and designed the experiments, performed the experiments, analyzed the data, wrote the paper, prepared figures, reviewed drafts of the paper, redid the experiments, and revised the paper. Y.H., D.X., and E.L. repeated the experiments, analyzed the data, and reviewed drafts of the paper. X.Y. and Y.H. performed the experiments and reviewed drafts of the paper. W.Z. and Q.W. contributed materials and reviewed drafts of the paper. J.G.W. conceived and designed the experiments, got the financial supports from the Foundations, provided the experimental platform and equipment, and reviewed drafts of the paper.

ADDITIONAL INFORMATION

The online version of this article (https://doi.org/10.1038/s41390-020-01329-x) contains supplementary material, which is available to authorized users.

Competing interests: The authors declare no competing interests.

Patient consent: Patient consent was not required.

Publisher's note Springer Nature remains neutral with regard to jurisdictional claims in published maps and institutional affiliations.

REFERENCES

1. Amarenco, G., Sheikh Ismaël, S., Chesnel, C., Charlanes, A. & Breton, L. E. F. Diagnosis and clinical evaluation of neurogenic bladder. *Eur. J. Phys. Rehabil. Med.* **53**, 975–980 (2017).
2. Sripathi, V. & Mitra, A. Management of neurogenic bladder. *Indian J. Pediatr.* **84**, 545–554 (2017).
3. Johnston, A. W., Wiener, J. S. & Todd Purves, J. Pediatric neurogenic bladder and bowel dysfunction: will my child ever be out of diapers? *Eur. Urol. Focus* **6**, 838–867 (2020).
4. Huen, K. H., Nik-Ahd, F., Chen, L., Lerman, S. & Singer, J. Neomycin-polymyxin or gentamicin bladder instillations decrease symptomatic urinary tract infections in neurogenic bladder patients on clean intermittent catheterization. *J. Pediatr. Urol.* **15**, 178.e1–178.e7 (2019).
5. Stein, R. et al. EAU/ESPU guidelines on the management of neurogenic bladder in children and adolescent part I diagnostics and conservative treatment. *Neurourol. Urodyn.* **39**, 45–57 (2020).
6. Tuite, G. F. et al. Lack of efficacy of an intradural somatic-to-autonomic nerve anastomosis (Xiao procedure) for bladder control in children with myelomeningocele and lipomyelomeningocele: results of a prospective, randomized, double-blind study. *J. Neurosurg. Pediatr.* **18**, 150–163 (2016).
7. de Barros, R. S. M. et al. Morphofunctional evaluation of end-to-side neurorrhaphy through video system magnification. *J. Surg. Res.* **221**, 64–68 (2018).
8. Gao, W., Liu, Q., Li, S., Zhang, J. & Li, Y. End-to-side neurorrhaphy for nerve repair and function rehabilitation. *J. Surg. Res.* **197**, 427–435 (2015).
9. Lai, J. et al. Activation of NFKB-JMJD3 signaling promotes bladder fibrosis via boosting bladder smooth muscle cell proliferation and collagen accumulation. *Biochim. Biophys. Acta.* **1865**, 2403–2410 (2019).
10. Li, Y. L. et al. Reconstruction of bladder function and prevention of renal deterioration by means of end-to-side neurorrhaphy in rats with neurogenic bladder. *Neurourol. Urodyn.* **37**, 1272–1280 (2018).
11. Tohru, T., Kazuki, U. & Akiyoshi, K. End-to-end and end-to-side neurorrhaphy between thick donor nerves and thin recipient nerves: an axon regeneration study in a rat model. *Neural Regen. Res.* **13**, 699–703 (2018).
12. Naqvi, S., Clothier, J., Wright, A. & Garriboli, M. Urodynamic outcomes in children after single and multiple injections for overactive and low compliance neurogenic bladder treated with abobotulinum toxin A. *J. Urol.* **203**, 413–419 (2020).
13. Doyle, C. et al. The role of the mucosa in modulation of evoked responses in the spinal cord injured rat bladder. *Neurourol. Urodyn.* **37**, 1583–1593 (2018).
14. Liu, Q., Wang, R., Wang, C., Li, Y. & Li, A. The protective role of Schwann cells in bladder smooth muscle cell fibrosis. *Int. J. Clin. Exp. Pathol.* **12**, 3799–3806 (2019).
15. Lu, Y. T., Tingskov, S. J., Djurhuus, J. C., Nørregaard, R. & Olsen, L. H. Can bladder fibrosis in congenital urinary tract obstruction be reversed? *J. Pediatr. Urol.* **13**, 574–580 (2017).
16. Şekerci, Ç. A. et al. Urinary NGF, TGF-beta1, TIMP-2 and bladder wall thickness predict neurourological findings in children with myelodysplasia. *J. Urol.* **191**, 199–205 (2014).
17. Zou, L. X. et al. Resveratrol attenuates pressure overload-induced cardiac fibrosis and diastolic dysfunction via PTEN/AKT/Smad2/3 and NF-kappaB signaling pathways. *Mol. Nutr. Food Res.* **63**, e1900418 (2019).
18. Tang, W. B. et al. Effect of pressure on liver stiffness during the development of liver fibrosis in rabbits. *Ultrasound Med. Biol.* **42**, 282–289 (2016).
19. Huang, Y. et al. Collagen type VI alpha 3 chain promotes epithelial-mesenchymal transition in bladder cancer cells via transforming growth factor beta (TGF-beta)/Smad pathway. *Med. Sci. Monit.* **24**, 5346–5354 (2018).
20. Liang, R., Fisher, M., Yang, G., Hall, C. & Woo, S. L. Alpha1,3-galactosyltransferase knockout does not alter the properties of porcine extracellular matrix bioscaffolds. *Acta Biomater.* **7**, 1719–1727 (2011).
21. Jiang, X. et al. Sodium tanshinone IIA sulfonate ameliorates bladder fibrosis in a rat model of partial bladder outlet obstruction by inhibiting the TGF-β/Smad pathway activation. *PLoS ONE* **10**, e0129655 (2015).